JOURNAL OF MAGNETIC RESONANCE 90, 52–70 (1990)

Optimization of Eddy-Current Compensation*

J. J. VAN VAALS† AND A. H. BERGMAN

Philips Research Laboratories, Building WAE, P.O. Box 80000, 5600 JA Eindhoven, The Netherlands

Received December 28, 1989; revised March 8, 1990

A comprehensive method for optimizing the preemphasis applied to pulsed gradients in NMR experiments in order to compensate induced eddy-current fields is presented. First, the eddy-current effects are measured without any compensation active. The eddy-current fields with spatial symmetries different from those of the pulsed gradient are also taken into account. Next, the measured response functions are analyzed with exponentially decaying terms. An exact solution of the required compensation is provided by numerical inversion of the response function using Laplace transformation. The calculated compensation terms are implemented in hardware. This yields a highly improved suppression of the eddy-current effects, including induced fields with spatial symmetries different from those of the switched gradient. The result is independent of the waveform or timing of the pulsed gradient and can compete with shielded gradient systems. © 1990 Academic Press, Inc.

Eddy-current fields are a major problem associated with switching magnetic field gradients in NMR imaging (*1*) and localized spectroscopy (*2*) sequences. They are induced when there are conducting structures present in the pulsed magnetic field, such as cryostat shields in superconducting magnets, Faraday screens, the main magnet windings, the shim coils, other gradient coils, or the RF coils (*3, 4*). The eddy currents will produce magnetic fields opposing the pulsed field, and will persist, decaying multiexponentially, for hundreds of milliseconds after switching the gradient on or off (*5, 6*). In consequence, the intended phase encoding of the magnetic spins will be distorted and there will be phase dispersion even when the gradients are switched off. This results in poor selective excitation, imperfect rephasing of echoes, loss of signal, and distorted images and spectra.

Apart from an eddy-current field with the same spatial symmetry as that of the pulsed linear gradient, eddy currents which generate fields with other spatial symmetries are often induced. Approximately, using the "method of images" well known from classical electrodynamics, the eddy-current field can be described as produced by a virtual current pattern which is the image of the gradient windings with respect to e.g., the cryostat shield cylinder. Because the gradient windings are designed for optimum linearity, and since this pattern is imaged by the cryostat shield mainly in the radial direction and not in the axial direction, the resulting fictitious current pattern will not

* Presented in preliminary form at the Eighth Annual Meeting of the Society of Magnetic Resonance in Medicine, Amsterdam, August 1989.

† To whom correspondence should be addressed at present address: Philips Medical Systems, Building QR, P.O. Box 10000, 5680 DA Best, The Netherlands.

0022-2364/90 $3.00

produce a perfect linear gradient field. Therefore, and due to coupling with other gradient or shim coils (which should be disconnected when not in use), higher-order terms may become important.

Also, eddy currents which produce a time-dependent but spatially invariant B_0 field shift, which is named a z_0 eddy-current field, can be induced. This asymmetry effect is the consequence of eccentric positioning of the internal radiation shields of the magnet with respect to the gradient bore. The gradient coil and all relevant cryostat shields must be positioned isocentrically by mechanical adjustment when possible.

Several methods for (partially) preventing or overcoming the eddy-current effects are proposed in the literature. The problem is alleviated when yokeless ferrite permanent magnets or specially designed superconducting magnets are used (*7*). Employing shaped gradient pulses is sequence dependent and deficient especially for the first 10–20 ms following the pulsed gradient (*8*). The most promising solution, shielded gradients (*9–13*), has the disadvantage of reduced bore size and will not prevent eddy-current fields originating from lossy structures inside the gradient coil, such as Faraday screen, RF coil, and conductive probe casing. The method employed in most NMR systems is the so-called preemphasis: the linear eddy-current fields are compensated by adding an overshoot to the waveform of the pulsed gradient (*14, 15*).

The z_0 eddy-current field can be reduced by separate compensation of the two halves of the gradient coil (*16*), but this impairs the linearity of the gradient. Alternatively, after data collection, the z_0 shift can be corrected by software using a previously determined phase-shift function (*17, 18*), which has the disadvantage of timing and sequence dependency. The best solution is to apply an exponentially decaying current to the z_0 (shim) coil (*19, 20*).

We present a comprehensive algorithm for measuring all eddy-current fields and optimizing the widely used overshoot compensation, resulting in a greatly improved suppression of the eddy-current effects. This is achieved by calculating exactly the required correction, taking into account the eddy currents induced by the overshoot correction itself, and by including the correction of eddy currents with spatial symmetries different from those of the pulsed gradient.

THEORY

The spatial symmetries of the pulsed magnetic gradient fields and the induced eddy-current fields are indicated by p and q, respectively, where p and q represent field symmetries corresponding to a set of shimming gradients:

$$p = x, y, z, z_0, xy, \ldots \quad \text{and} \quad q = x, y, z, z_0, xy, \ldots. \qquad [1]$$

The z component of the induced magnetic eddy-current field can be developed in q terms with amplitudes $c_q(t)$:

$$B_z(\mathbf{r}, t) = \sum_q c_q(t) q. \qquad [2]$$

Each q term is induced by pulsed magnetic fields with spatial symmetry p:

$$c_q(t) = \sum_p B_{pq}(t). \qquad [3]$$

Thus, the time-dependent eddy-current field is described by a set of functions $B_{pq}(t)$, where each $B_{pq}(t)$ specifies the q eddy-current field after pulsing a p gradient:

$$B_z(\mathbf{r}, t) = \sum_{p,q} B_{pq}(t)q. \qquad [4]$$

To analyze the functions $B_{pq}(t)$, we consider a set of LR circuits representing the conducting structures of the NMR system in which the eddy currents are induced (see Fig. 1). Each subset of n_{pq} circuits is responsible for the generated eddy-current fields with spatial symmetry q. All circuits are mutually coupled with the gradient-coil circuit and with the other eddy-current circuits. Therefore, the eddy currents I_{qi} in the circuits q, i are given by a set of $n_{pq_0} + n_{pq_1} + \cdots + n_{pq_j}$ differential equations:

$$R_{qi}I_{qi} + L_{qi}\frac{dI_{qi}}{dt} + M_{qi}^{p}\frac{dI_p}{dt} + \sum_{j\neq i}^{n_{pq}} M_{qi}^{qj}\frac{dI_{qj}}{dt} + \sum_{q'\neq q}\sum_{j=1}^{n_{pq'}} M_{qi}^{q'j}\frac{dI_{q'j}}{dt} = 0 \qquad [5]$$

for each q, i (where $q = q_0, q_1, \ldots, q_j$ and $1 \leqslant i \leqslant n_{pq}$). After pulsing the gradient p with the step function

$$I_p = \begin{cases} 0 & \text{for } t < 0 \\ I_0 & \text{for } t > 0 \end{cases} \qquad [6]$$

the solution of the above set of equations for the induced eddy current in the circuit q, i is

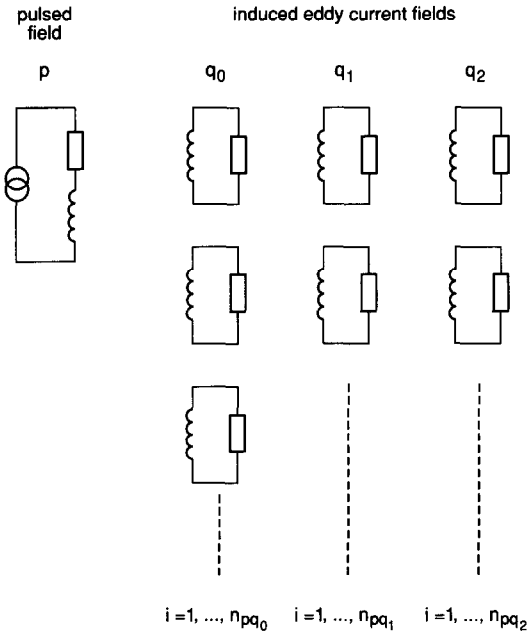

FIG. 1. After pulsing a gradient field p, eddy currents are induced in conducting structures of the NMR system which can be described by a set of LR circuits. All circuits are mutually coupled.

$$I_{qi}(t) \propto -I_0 b_i^{pq} e^{-t/T_i^{pq}}. \quad [7]$$

So, the eddy-current field described by $B_{pq}(t)$ is specified by a discrete sum of exponentially decaying terms for each spatial symmetry q:

$$B_{pq}(t) \propto \sum_{i=1}^{n_{pq}} a_i^{pq} e^{-t/T_i^{pq}}. \quad [8]$$

The ratio a_i^{pq}/b_i^{pq} depends on the efficiency for generating a field when current is induced in the circuit q, i. For each circuit, this ratio, R_{qi}, and L_{qi} are dependent on the resistivity of the conducting structure and on geometric factors. Due to the coupling between, in principle, all the circuits (when not orthogonal), the amplitude a_i^{pq} and time constant T_i^{pq} for the eddy-current field generated by a specific circuit are a complex function of the parameters of all the circuits. Fortunately, it is not required for the calculation of the eddy-current compensation to have any knowledge at all of the values of R_{qi} and L_{qi} of the individual circuits, their mutual coupling constants, or the efficiency ratios a_i^{pq}/b_i^{pq}.

We will now describe the mathematical method for an exact solution of the eddy-current compensation, taking intrinsically into account all mutual couplings, including the additional eddy currents introduced by the correction, and including the eddy-current fields with spatial symmetry different from the pulsed gradient. This is done by first describing a system without any compensation active, then by considering a system with only compensation for the diagonal terms, and finally by solving the problem of compensation including cross-terms.

No compensation. The technique of signal-processing analysis, employing a mathematical description and representation of signals and systems, is an excellent tool for our problem, and can be used since an NMR system is a time-invariant system with linear response. Using this method, the induced field is described by the convolution of the input current of the gradient amplifier with a system impulse-response function. Compensation circuits are simply electronic filters with a specific impulse response, and, when implemented, are included in the convolution. Mathematically, the solution is most easily obtained by considering the transfer function, which is the Laplace transform of the impulse-response function. The signal-analysis technique is described educationally and in condensed form by Oppenheim *et al.* (*21*). Useful properties of Laplace transforms are given, e.g., in Refs. (*21, 22*).

Consider a system in which eddy currents are induced, but where no compensation is active.[1] A pictorial representation is shown in Fig. 2. After pulsing a p or q gradient, eddy-current fields with the same spatial symmetry are induced, denoted by B_{pp} and B_{qq}. Moreover, after pulsing the p gradient, eddy currents are induced generating a field with q spatial symmetry, specified by B_{pq}. So, as an example, this is an NMR system with not only diagonal-term but also cross-term eddy-current fields.

The system inputs are the gradient input currents $I_p(t)$ and $I_q(t)$, and the system outputs are the induced fields described by $B_{pp}(t)$, $B_{pq}(t)$, and $B_{qq}(t)$. The system

[1] To prevent confusion by mixing up the current i and the subscript i in the first part of this publication, we reversed the usual notation in signal-analysis techniques. In our notation, which is compatible with the convention of Ref. (*22*), capitals denote the original functions in the time domain, and lowercase characters are reserved for their Laplace transform image functions in the s domain.

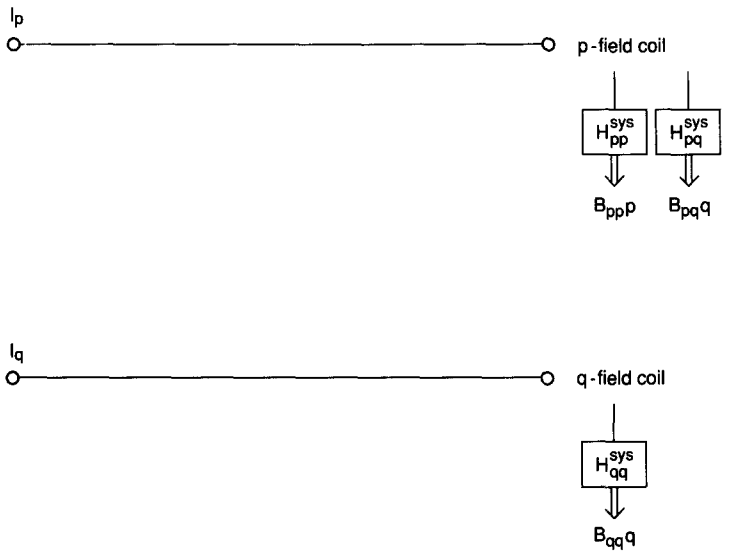

FIG. 2. System with diagonal ($p \rightarrow p$ and $q \rightarrow q$)- and cross-term ($p \rightarrow q$) eddy-current fields; no eddy-current compensation active.

impulse-response functions $H_{pp}^{sys}(t)$, $H_{pq}^{sys}(t)$, and $H_{qq}^{sys}(t)$ give the relation between input and output, describing the interaction of the gradient coil with the rest of the NMR system. These functions therefore specify the induced fields, including the mutual coupling between all conducting structures in which eddy currents are induced.

In general, for both diagonal terms and cross terms, the induced eddy-current fields are given by convolving the input current with the impulse-response function of the system,

$$I_p(t) \circledast H_{pq}^{sys}(t) = B_{pq}(t) \xrightarrow{\mathcal{L}} i_p(s)h_{pq}^{sys}(s) = b_{pq}(s), \qquad [9]$$

with p and q any spatial symmetry, and where $\mathcal{L}$ is the Laplace transform operator and $i_p(s)$, $h_{pq}^{sys}(s)$, and $b_{pq}(s)$ are the image functions of $I_p(t)$, $H_{pq}^{sys}(t)$, and $B_{pq}(t)$, respectively.

For an ideal system, the generated magnetic field does not deviate from the input current waveform, so

$$H_{pq}^{sys}(t) = \delta_{pq}\delta(t) \xrightarrow{\mathcal{L}} h_{pq}^{sys}(s) = \delta_{pq}. \qquad [10]$$

For a nonideal system this is not valid for all $q = p$ and some $q \neq p$, as a consequence of induced eddy currents. For the calculation of the required compensation, the system impulse-response functions $H_{pq}^{sys}(t)$ must be determined. This can be done by applying, without any compensation active, the Heaviside unit step function $U(t)$ as input current $I_p(t)$:

$$I_p(t) = U_p(t) = \begin{cases} 0 & \text{for } t < 0 \\ \frac{1}{2} & \text{for } t = 0 \\ 1 & \text{for } t > 0 \end{cases} \xrightarrow{\mathcal{L}} u_p(s) = \frac{1}{s}. \qquad [11]$$

Then the field $B_{pq}(t)$ is by definition the step-response function $G_{pq}(t)$ and can be measured:

$$B_{pq}(t) = G_{pq}(t) = \delta_{pq} - \sum_{i=1}^{n_{pq}} a_i^{pq} e^{-t/T_i^{pq}} \qquad \text{for } t > 0$$

$$\xrightarrow{\mathcal{L}} \quad g_{pq}(s) = \frac{1}{s}\,\delta_{pq} - \sum_{i=1}^{n_{pq}} \frac{a_i^{pq}}{s + w_i^{pq}} \qquad \text{with } w_i^{pq} \equiv \frac{1}{T_i^{pq}}\,. \qquad [12]$$

The amplitudes a_i^{pq} and time constants T_i^{pq} are experimentally determined by an n_{pq}-exponential fit of the eddy-current fields in a system without any compensation active, measured after applying a step function as input current. The system impulse-response function follows from Eq. [9]:

$$h_{pq}^{\text{sys}}(s) = \frac{b_{pq}(s)}{i_p(s)} = \frac{g_{pq}(s)}{u_p(s)}\,. \qquad [13]$$

Substitution of Eqs. [11] and [12] yields

$$h_{pq}^{\text{sys}}(s) = sg_{pq}(s) = \delta_{pq} - \sum_{i=1}^{n_{pq}} \frac{a_i^{pq} s}{s + w_i^{pq}}\,. \qquad [14]$$

The transfer function $h_{pq}^{\text{sys}}(s)$ is now determined and can be used for the calculation of the required compensation, as will be demonstrated below.

Compensation excluding cross terms. In Fig. 3 a schematic diagram of the same system is shown, but now with compensation filters for the diagonal terms, characterized by the correction impulse-response functions $H_{pp}^{\text{cor}}(t)$ and $H_{qq}^{\text{cor}}(t)$. The induced fields are now described by

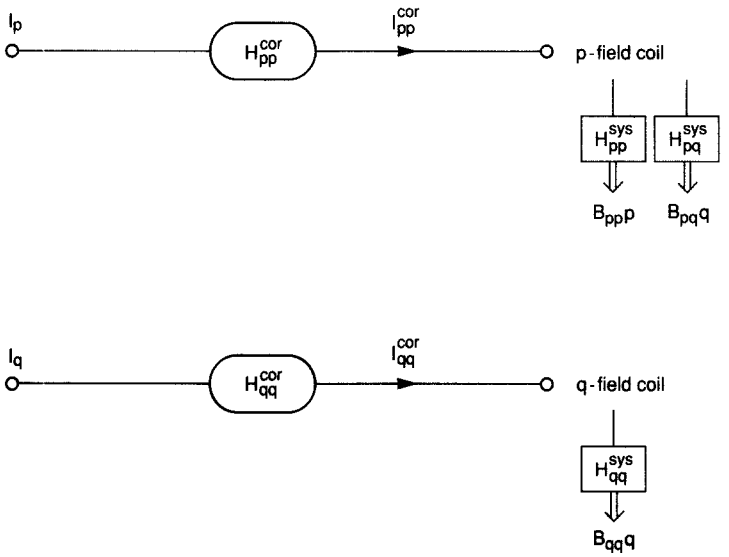

FIG. 3. System with diagonal ($p \rightarrow p$ and $q \rightarrow q$)- and cross-term ($p \rightarrow q$) eddy-current fields; eddy-current compensation excluding cross terms implemented.

$$I_p(t) \circledast H_{pp}^{\text{cor}}(t) = I_{pp}^{\text{cor}}(t) \qquad \text{and} \qquad I_{pp}^{\text{cor}}(t) \circledast H_{pq}^{\text{sys}}(t) = B_{pq}(t), \qquad [15]$$

where $I_{pp}^{\text{cor}}(t)$ describes the waveform of the input current including the overshoot correction imposed by the compensation circuit. By combining Eqs. [15],

$$I_p(t) \circledast H_{pp}^{\text{cor}}(t) \circledast H_{pq}^{\text{sys}}(t) = B_{pq}(t), \qquad [16]$$

it can be seen that exact compensation for the diagonal terms ($q = p$) is achieved when

$$H_{pp}^{\text{cor}}(t) \circledast H_{pp}^{\text{sys}}(t) = \delta(t) \xrightarrow{\mathcal{L}} h_{pp}^{\text{cor}}(s) h_{pp}^{\text{sys}}(s) = 1. \qquad [17]$$

So the transfer function of the filter must be the inverse of the transfer function of the system. The specification for the correction filters is obtained by calculating the corrected current $I_{pp}^{\text{cor}}(t)$. Using Eqs. [15] and [17] it follows that for exact correction,

$$i_{pp}^{\text{cor}}(s) = i_p(s) h_{pp}^{\text{cor}}(s) \qquad \text{and} \qquad h_{pp}^{\text{cor}}(s) = \frac{1}{h_{pp}^{\text{sys}}(s)}. \qquad [18]$$

With the unit step function as the input current (Eqs. [11]), and using the transfer function of the system which we calculated in the previous section (Eq. [14]), we find

$$i_{pp}^{\text{cor}}(s) = \frac{i_p(s)}{h_{pp}^{\text{sys}}(s)} = \frac{u_p(s)}{s g_{pp}(s)} = \frac{1}{s(1 - \sum_{i=1}^{n} (a_i s/(s + w_i)))}, \qquad [19]$$

where for notational convenience the super- and subscript pp is dropped on the eddy-current parameters: $a_i \equiv a_i^{pp}$, $w_i \equiv w_i^{pp} \equiv 1/T_i^{pp}$, and $n \equiv n_{pp}$. Next, parameters p_k are defined by

$$p_k \equiv \sum_{j_1 \neq j_2 \neq \cdots \neq j_{n-k}=1}^{n} \frac{w_{j_1} w_{j_2} w_{j_{n-k}}}{(n-k)!}, \qquad [20]$$

which is equivalent to (with $p_k^{(n)} = p_k$ for $k_{\max} = n$)

$$\begin{aligned} p_0^{(n)} &= \prod_{i=1}^{n} w_i \\ p_k^{(n)} &= p_{k-1}^{(n-1)} + w_n p_k^{(n-1)} \qquad \text{for } 0 < k < n \\ p_n^{(n)} &= 1; \end{aligned} \qquad [21]$$

and parameters q_k are defined by

$$q_k \equiv p_k - \sum_{i=1}^{n} a_i p_k^{[i]}, \qquad [22]$$

where $p_k^{[i]}$ is p_k calculated with w_i set at zero. Using the parameters p_k and q_k, we rewrite the image function $i_{pp}^{\text{cor}}(s)$, where $\prod^{[i]}$ denotes the product of all but the ith term:

$$i_{pp}^{\mathrm{cor}}(s) = \frac{\prod_{i=1}^{n}(s+w_i)}{s\{\prod_{i=1}^{n}(s+w_i) - \sum_{i=1}^{n} a_i s \prod_{k=1}^{n\ [i]}(s+w_k)\}}$$

$$= \frac{\sum_{k=0}^{n} p_k s^k}{\sum_{k=0}^{n} q_k s^{k+1}}$$

$$= \frac{\sum_{k=0}^{n} p_k s^k}{\prod_{k=0}^{n}(s+\Omega_k)} = \sum_{i=0}^{n} \frac{\alpha_i}{s+\Omega_i}. \qquad [23]$$

Thus $i_{pp}^{\mathrm{cor}}(s)$ is determined by the poles $\Omega_i \equiv \Omega_i^{pp} \equiv 1/\tau_i^{pp}$, which are the roots of the polynomial

$$\sum_{k=0}^{n} q_k s^{k+1}, \qquad [24]$$

and the residues $\alpha_i \equiv \alpha_i^{pp}$, which are given by

$$\alpha_i = \frac{\sum_{k=0}^{n} p_k(-\Omega_i)^k}{\prod_{k=0}^{n\ [i]}(\Omega_k - \Omega_i)}. \qquad [25]$$

Finally, with $\Omega_0 = 0$ and $\alpha_0 = 1$, it is found that

$$i_{pp}^{\mathrm{cor}}(s) = \frac{1}{s} + \sum_{i=1}^{n} \frac{\alpha_i}{s+\Omega_i}. \qquad [26]$$

Now, inverse Laplace transformation gives the corrected current (when the unit step function is applied as input current) required for exact compensation of the eddy-current field with the same spatial symmetry as that of the pulsed field:

$$I_{pp}^{\mathrm{cor}}(t) = \begin{cases} 0 & \text{for } t < 0 \\ 1 + \sum_{i=1}^{n_{pp}} \alpha_i^{pp} e^{-t/\tau_i^{pp}} & \text{for } t \geqslant 0. \end{cases} \qquad [27]$$

So, for exact correction of the diagonal eddy currents the filter must convolve the waveform of the current delivered to the filter with the simple multiexponentially decaying part of the above function. The filter function is specified by n_{pp} decaying exponentials with amplitudes α_i^{pp}, which are the residues α_i^{pp} calculated with Eq. [25], and with time constants τ_i^{pp}, given by the inverse of the roots Ω_i^{pp} which are calculated from Eq. [24].

Compensation including cross terms. Now the correction of cross terms is also included, as depicted in Fig. 4. In this figure several alternative pathways are suggested which can be used when filters for the correction of the cross terms are implemented. For diagonal terms ($q = p$), the induced fields and the condition for exact compensation are, for this scheme, also described by Eqs. [16] and [17]. The required compensation for the diagonal terms is not affected by the correction of the cross terms and is calculated in the previous section. For cross terms ($q \neq p$), the most straightforward way of compensating is to use version (a) of correcting a cross term, indicated in Fig. 4 by the correction filter with impulse-response function $H_{pq}^{\mathrm{cor(a)}}$. In that case, after pulsing an input current $I_p(t)$, the q field generated by the current applied to the p-field gradient coil is denoted by $B_{pq}(t)$ and is given by

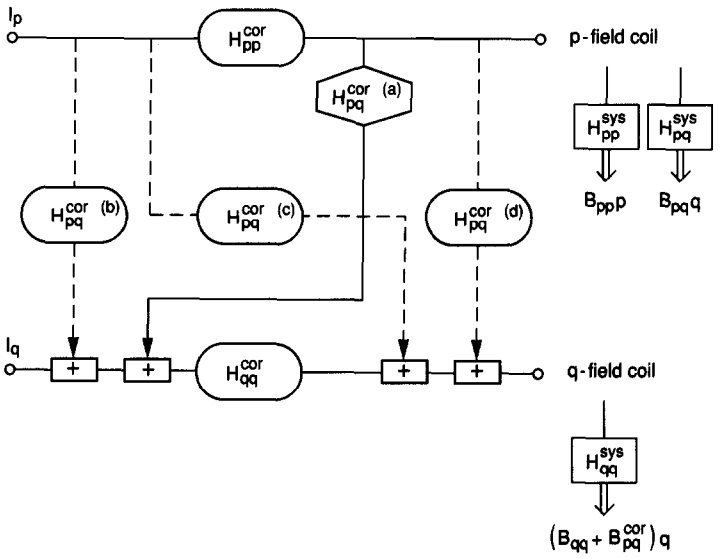

FIG. 4. System with diagonal ($p \rightarrow p$ and $q \rightarrow q$)- and cross-term ($p \rightarrow q$) eddy-current fields; eddy-current compensation including cross terms implemented.

$$I_p(t) \otimes H_{pp}^{\mathrm{cor}}(t) \otimes H_{pq}^{\mathrm{sys}}(t) = B_{pq}(t), \qquad [28]$$

and the q field generated by the current which is, through the cross-term correction circuit, applied to the q-field gradient coil is denoted by $B_{pq}^{\mathrm{cor}}(t)$ and is described by

$$I_p(t) \otimes H_{pp}^{\mathrm{cor}}(t) \otimes H_{pq}^{\mathrm{cor(a)}}(t) \otimes H_{qq}^{\mathrm{cor}}(t) \otimes H_{qq}^{\mathrm{sys}}(t) = B_{pq}^{\mathrm{cor}}(t). \qquad [29]$$

The cross terms will be exactly compensated when

$$B_{pq}^{\mathrm{cor}}(t) = -B_{pq}(t). \qquad [30]$$

Since the diagonal term for the q gradient is compensated according to the condition of Eq. [17], it follows from Eqs. [28]–[30] that

$$H_{pq}^{\mathrm{cor(a)}}(t) = -H_{pq}^{\mathrm{sys}}(t). \qquad [31]$$

Therefore, using compensation of the cross terms according to scheme (a) of Fig. 4, the correction filter must simply pass a waveform which is opposing but shaped identically to the cross-term step response measured in the absence of any compensation. In other words, for exact compensation the correction circuits for the cross terms must convolve the current which is applied to the filter with the negative of a multiexponentially decaying function specified by the n_{pq} exponentials with parameters a_i^{pq} and T_i^{pq} describing the induced cross-term eddy-current fields measured without compensation active.

When an alternative scheme for the correction of cross-terms is used, for instance, any of the schemes (b)–(d) indicated in Fig. 4, or when not only $p \rightarrow q$ but also the reverse $q \rightarrow p$ eddy-current fields are induced, the required compensation can be calculated by a completely similar mathematical approach.

A computer program for calculating exactly the required eddy-current compensation

from noncompensated eddy-current field parameters was developed, employing the method described above. The inverse calculation is also implemented. For interested readers the Fortran source program is available upon request.

OPTIMIZATION ALGORITHM

The successive steps of measuring and quantifying the induced eddy-current fields and of calculating and implementing the correction required for exact compensation are now discussed.

First the eddy-current fields following excitation with a step function are measured without any compensation active. Usually, this is done with small pick-up coils or tiny NMR samples. In that case, for a complete analysis of all the possible spatial symmetries, the eddy-current fields must be measured typically at 31 points, from which the spatial dependence is determined using field-analysis methods employing Legrende polynomials or spherical harmonics (*23, 24*). This must be done at a number of points in time to obtain the time dependence. However, less laborious methods are usually practiced: the single-point measurement method which is insensitive to or disturbed by eddy-current fields with nondiagonal spatial symmetry, or the often used two-point method which has similar problems but eliminates or gives information on the z_0 eddy-current fields. So, employing a point method, complete analysis requires measurements at many spatial points, whereas when the measurements are confined to one or two points eddy-current fields with other symmetries simultaneously present are either overlooked or contaminate the information measured for the diagonal eddy-current field.

Alternatively, we use a phantom which more or less covers the complete volume of interest in order to consistently determine all the eddy-current fields, including those with spatial symmetry different from that of the pulsed gradient. Initially, the magnetic field homogeneity is optimized without any gradient being pulsed. Then the eddy-current fields are measured with the pulse sequence depicted in Fig. 5 by adjusting the shims to maximize the observed FID for given delay times δ following a p gradient pulse. This will be possible with just the p shim when only eddy-current fields with p spatial symmetry are induced. When, however, cross-term eddy-current fields are significant, maximizing the FID will not be feasible with only the diagonal shim, and the shims corresponding to the cross-term spatial symmetries must be included in the procedure. So with this method the presence of relevant cross-term eddy-current fields is instantly noticed, and they are measured simultaneously with but independently of the diagonal term.

FIG. 5. Pulse sequence for measuring eddy-current fields. The pulsed gradient is switched on during a time Δ which is at least five times the largest eddy-current time constant T^{pq}_{max}. The fall time of the gradient must be as short as possible. The delay time δ is variable. The RF pulse excites the nuclear spins with a small tip angle. The NMR signal is real-time displayed on a large screen monitor or numerically evaluated in order to allow interactive optimization of the individual shims for a specific time δ.

The gradient is switched on for a long time Δ, typically 3 s, but at least five times the largest eddy-current time constant $T_{\max}^{pq}$. The fall time t_f of the gradient must be as short as possible since the method described under Theory demands excitation of the eddy-current fields with a step function. In practice the nonzero fall time, which is typically 0.5–1 ms, causes only very small errors in the measured eddy-current amplitudes $a_{i,\text{meas}}^{pq}$:

$$a_i^{pq} = a_{i,\text{meas}}^{pq}\left(1 + \frac{1}{24}\left(\frac{t_f}{T_i^{pq}}\right)^2 + \cdots\right). \qquad [32]$$

So the amplitude will be affected by less than 0.5% when $T_i^{pq} > 3t_f$. The determination of the eddy-current time constants is not impaired at all by a nonzero fall time. Only the first part of $\approx$10 ms of the FID is observed. The procedure is repeated for several values of δ. For small δ and strong eddy-current fields, maximization is only possible for the first few milliseconds of the FID. The NMR signal is acquired off resonance in order to separate the effect of a frequency shift as a consequence of a z_0 eddy-current field, and of a change in the envelope as a result of eddy-current fields with any other spatial symmetry.

Next, the observed eddy-current behavior as a function of time following the p gradient pulse is fitted for each spatial dependence q with n_{pq} exponential terms (see Eq. [12]). The accuracy of the parameters determined by the fit procedure is essential for the result of the calculation of the correction constants.

Then, the compensation required for exact correction is calculated both for diagonal and for cross terms with the method described under Theory. The step response of the system is measured more easily after the gradient is switched off, as described above, whereas the theory describes the situation after switching the gradient on more conveniently. This is no problem since the induced eddy-current fields in both situations are opposite but identically shaped.

Finally, the calculated overshoot exponentials are implemented in the hardware, e.g., using the well-known circuit for a multiexponentially decaying overshoot given in Fig. 6, where R_i^a, and R_i^c set amplitude and time constant independently for each exponential term:

$$a_i^{pq} = \frac{R_i^a R^r}{R_i^{a,\max}(R_i^a + R_i^b) - R_i^{a2}} \approx \frac{R_i^a}{R_i^{a,\max}}\frac{R^r}{R_i^b} \qquad \text{for } R_i^a \ll R_i^b, \qquad [33]$$

$$T_i^{pq} = R_i^c C_i. \qquad [34]$$

For diagonal terms ($q = p$), the amplitude and time constant are of course defined by α_i^{pp} and τ_i^{pp}. The maximum adjustable amplitude and time constant are limited by R^r/R_i^b and by $R_i^{c,\max}C_i$, respectively. By splitting up the resistors R_i^a and R_i^c, the lower limit can also be set in order to allow more accurate setting of the parameters. The resistor R_0^b is only inserted for diagonal filters, where the ratio R^r/R_0^b determines the sensitivity for passing the original waveform. It can be convenient when this ratio deviates from one, for instance, for the $pq = z_0z_0$ filter. Because the accuracy of the correction established with the compensation algorithm described is very high, also the temperature and time stability of the electronic components must be high to ensure proper functioning of the eddy-current compensation over a longer time period.

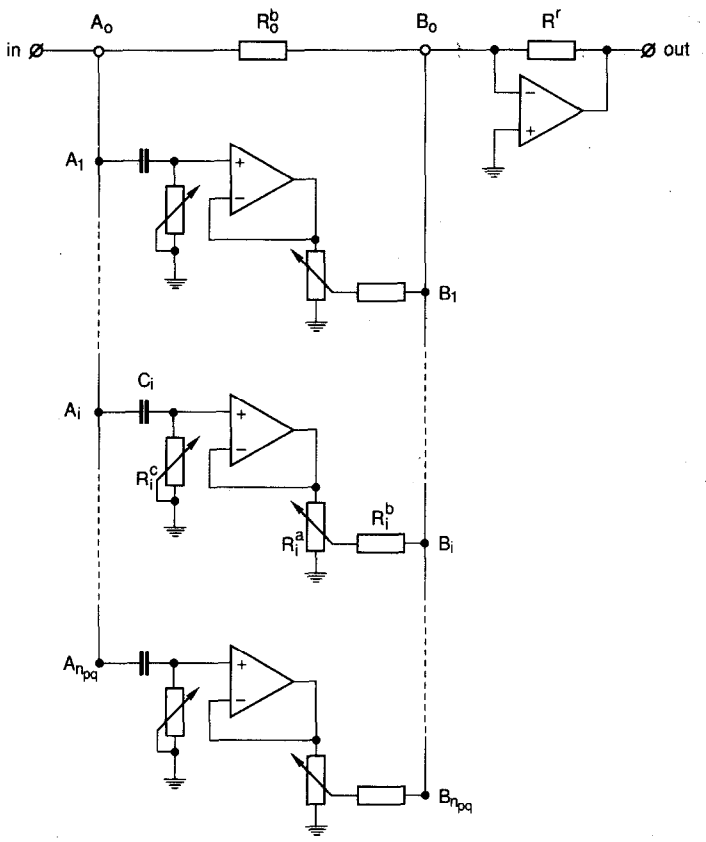

FIG. 6. Electronic correction filter compensating q eddy-current fields after pulsing a p gradient. The basic circuits connected between A_i and B_i (with $i = 1, \ldots, n_{pq}$) induce exponentially decaying overshoots with amplitudes and time constants independently set by R_i^a and R_i^c, respectively. The resistor R_0^b is only inserted between A_0 and B_0 for diagonal filters ($q = p$).

To facilitate the setting of the exponential parameters, the circuit of Fig. 6 can be adapted to allow computer control of the amplitudes and time constants, for example, using programmable switched-capacitor filters. Even more sophisticated is the use of computer-controlled digital signal-processing (DSP) techniques for the correction filters, which has the additional benefit of superior accuracy and stability.

When there are measurement or fitting errors, or errors as a consequence of tolerance in the amplifier and correction-circuit components, fine adjustment employing the measurement method described above may be required to give the optimum compensation. This is most easily done by starting with a large δ and first adjusting the amplitude of the term with the largest time constant, and subsequently proceeding to shorter times δ and terms with smaller time constants.

Using the method of observing and optimizing the NMR signal of a large phantom with the shims, eddy-current fields with any spatial symmetry are inevitably noticed due to their effect on the NMR signal and instantly identified and quantified by the shims required for the optimization. Another advantage of this method is that the (residual) eddy-current fields are assessed by exactly the same criterion used when the

NMR imaging and spectroscopy results are evaluated, namely the spectral linewidth, shift, and shape observed over the volume of interest.

RESULTS

We used the novel algorithm to improve the eddy-current compensation of our 6.3 T, 20 cm horizontal-bore animal system with 20 T/m nonshielded gradients. The free bore of the Oxford Instruments magnet with the gradient and shim set inserted is 13.5 cm. In this system, the eddy currents induced immediately following a long gradient pulse ($\Delta \geq 5T_{\max}^{pq}$ and $\delta = 0$ in Fig. 5) are of the order of 45% of the pulsed gradient level, requiring a compensation overshoot of approximately 80% on the gradient waveform. The basic eddy-current time constants are of the order of 15, 130, and 600 ms. Table 1 gives a complete list of all the induced eddy-current fields, measured without any compensation active. Also listed are the parameters required for exact compensation, calculated by the computer program which determines the amplitudes and time constants according to the method reported under Theory, where for correction of the nondiagonal terms scheme (a) of Fig. 4 is assumed.

In Fig. 7 the block diagram for compensation of the 6.3 T animal system is shown.

TABLE 1

Eddy-Current Compensation Parameters[a] of a 6.3 T System

Pulsed field p	Induced field q	Response function[b] a_i^{pq}	Response function[b] T_i^{pq}	Required overshoot[c] α_i^{pq}	Required overshoot[c] τ_i^{pq}
x	x	2.60	7.0	11.73	6.6
		17.96	19.8	40.11	15.1
		14.45	102.9	19.31	86.9
		8.83	343.2	8.22	315.1
		0.59	6272.7	0.58	6236.0
	z_0	0.254	7.2	0.254	7.2
		0.126	73.1	0.126	73.1
y	y	22.85	18.0	57.56	12.5
		18.39	137.3	22.81	111.7
		4.59	624.8	4.24	597.8
	z	6.81	11.4	6.81	11.4
		6.46	107.3	6.46	107.3
	z_0	0.165	5.1	0.165	5.1
		0.296	165.8	0.296	165.8
z	z	17.06	16.5	27.29	13.3
		8.85	135.7	9.67	123.7
		2.22	866.3	2.18	847.5
z_0	z_0	42.37	3.0	191.05	1.3
		19.96	38.5	26.17	30.6
		6.82	404.3	6.93	377.4

[a] The unit of a_i^{pq} and α_i^{pq} is a percentage of the pulsed field p, except for $p \neq z_0$ and $q = z_0$ where the unit is ppm/(mT/m). The unit of T_i^{pq} and τ_i^{pq} is ms.

[b] Measured without any compensation active.

[c] For nondiagonal terms the compensation is implemented according to scheme (a) of Fig. 4.

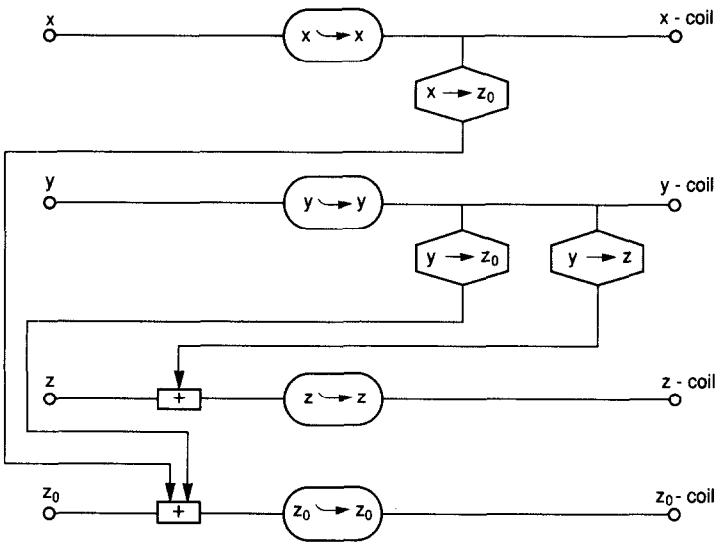

FIG. 7. Block diagram for eddy-current compensation of the 6.3 T, 20 cm diameter horizontal-bore Oxford Instruments magnet. Inserted are 13.5 cm diameter bore nonshielded gradients with maximum strength of 20 mT/m and minimum rise and fall time for pulsing between zero and maximum gradient strength of 1 ms.

In a preliminary attempt, we implemented 8–12 exponentials per correction filter, yielding maximum flexibility. We realized the circuit of Fig. 6, combining four basic circuits A_i–B_i at a time, by using a quad operational amplifier (Precision Monolithics, Inc., OP-400). After fine adjustment of the eddy-current compensation, the actual filter setting using an electronic filter with 12 exponential terms was measured and was found to be virtually identical to the calculated compensation described by n_{pq} terms (typically $n_{pq} = 3$) given in Table 1; the difference is less than the estimated level of residual eddy-current fields. So the n_{pq} calculated terms do indeed specify the required filter parameters with an excellent accuracy.

Implementing the calculated n_{pq}-exponential overshoot correction listed in Table 1 immediately reduced the eddy-current effects to less than 1%, which was improved easily by some additional fine tuning of the amplitudes. The initial accuracy is limited by the accuracy of the estimated uncorrected eddy-current parameters, and by inaccuracies in the hardware (accuracy of preemphasis settings and amplification parameters, amplifier stability and noise, and so on). Subsequent fine tuning of only the preset amplitudes resulted in residual eddy-current fields which are $\leq 0.25\%$ of the pulsed gradient for $\delta \geq 300$ μs and $\Delta = 3$ s, and $\leq 0.05\%$ of the pulsed gradient for $\delta \geq \Delta$ following a gradient pulse typically used in NMR experiments ($\Delta = 2$ ms). This is better, and much easier to realize, than the specifications for a shielded gradient set (with smaller bore) which was designed by an external company for our animal system.

The quality of the compensation is not destroyed by changing the magnitude or the rise or fall time of the pulsed gradient.

In Fig. 8 we illustrate the effect of eddy currents and the results with the optimized compensation on a 4 cm diameter spherical phantom covering the complete region

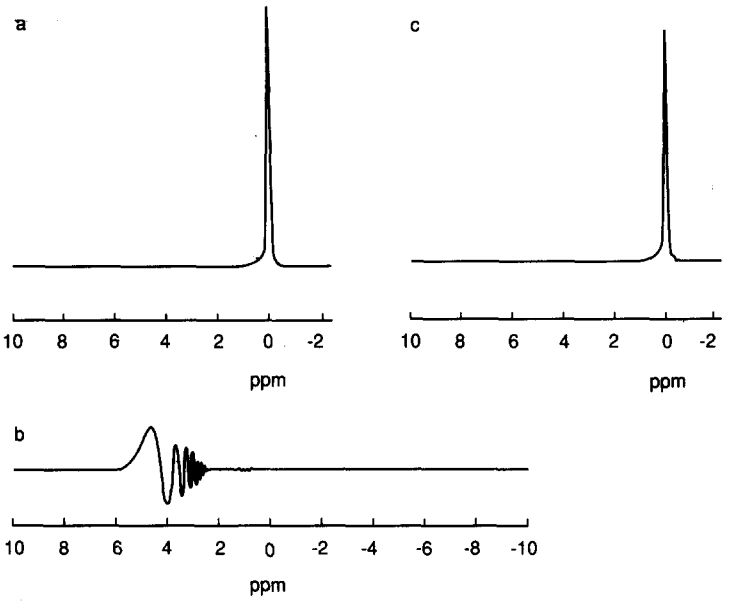

FIG. 8. The effect of eddy currents on a 15 Hz spectral line obtained from a 4 cm diameter spherical phantom covering the complete volume of interest in a 6.3 T horizontal-bore animal system. (a) No gradient pulsed. (b) With y gradient pulsed and with optimum compensation for $pq = yy$, but no compensation for cross terms. (c) With y gradient pulsed and with optimum compensation for $pq = yy$, $pq = yz$, and $pq = yz_0$. The signals are obtained using the pulse sequence described in Fig. 5, with the gradient switched on at a strength of 10 mT/m for a time $\Delta = 3$ s, with the fall time $t_f = 0.5$ ms, and start of data acquisition at a time $\delta = 1$ ms after the switching off of the gradient.

which is of interest in our animal system for imaging and spectroscopy of the rat. Figure 8a shows the Fourier transform of the NMR signal obtained from this phantom when no gradients are pulsed. The signal is shimmed to 15 Hz (0.06 ppm) which is a linewidth representative of metabolites in biological tissue at 6.3 T.

When only eddy-current fields with the same spatial symmetry as that of the pulsed gradient are corrected, still significant eddy-current fields are not compensated, as is clear from Fig. 8b, where a 10 mT/m y gradient was pulsed for 3 s, and switched off 1 ms prior to data acquisition. The y gradient pulse induces y, z, and z_0 eddy-current fields (see Table 1). If small pick-up coils or NMR samples had been used at one or more places along the y axis to measure the eddy-current fields following a y gradient pulse, the effect of the induced z eddy-current field would not have been noticed at all, and the z_0 eddy-current field only after special analyses. The spectral line is shifted 4.6 ppm (1240 Hz) downfield, indicating a strong z_0 eddy-current field. The "wiggles" are a consequence of the time dependence of the z_0 eddy-current field and of the presence of an eddy-current gradient field (*25*), obviously with a spatial symmetry different from that of the pulsed gradient.

Figure 8c shows the spectral line when the cross terms are also compensated. The spectrum is now almost completely free from eddy-current effects and appears nearly identical to the spectrum obtained when no gradient was pulsed.

DISCUSSION

The novel compensation algorithm improved the elimination of eddy-current effects dramatically. The method succeeded in reducing the residual eddy-current fields by a factor of at least five in systems which were initially optimally adjusted with conventional methods. This was established both in animal systems with horizontal 20 cm bore (6.3 T) and vertical 7 cm bore (7 T) and in a human whole-body 4 T system. In our 6.3 T, 20 cm diameter horizontal-bore Oxford Instruments magnet with 20 mT/m gradients, we reduced the eddy-current fields by a factor of $\approx$200 compared to the situation without any compensation, yielding residual eddy-current fields $\approx$400 times less strong than those of the pulsed gradient.

NMR results which were only obtainable after improving the eddy-current compensation according to our algorithm were presented in preliminary form at several meetings in 1988 (*26, 27*) and 1989 (*28–30*). Those results concern high-resolution imaging, spectroscopic imaging, and spectroscopy of very small volumes and will be the subject of future publications.

After we implemented the optimized compensation of the eddy currents in our 6.3 T system (*31*) and tested the result by localized spectroscopy investigations (*26, 27*), several publications appeared, disclosing related solutions to the problem (*14, 32, 15*). However, none of the published algorithms described the measurement method (sensitive to eddy-current fields with any spatial symmetry employing an NMR signal which at the same time reflects the final objective pursued) and comprehensive approach (yielding a complete and mathematically exact solution without any approximation for the compensation of all eddy-current fields, including mutual coupling and cross terms) as presented in this paper.

The reduction of eddy-current effects is at least as good as can be obtained with available double-shielded gradient sets, which have the disadvantage of smaller bore size or reduced gradient strength. In our system the uncompensated eddy-current fields are as large as 45% of the pulsed gradient. We have realized a reduction to residual effects of less than 0.5% of the uncompensated eddy-current fields, corresponding to 0.25% of the switched gradient, within 300 μs following the gradient pulse. The literature on self-shielded gradients reports a reduction relative to the uncompensated eddy-current fields down to 3–10% for single screening (*33, 34*) and a design specification of 1% for double screening (*35*), which can be improved by further optimalization. In practice, however, the elimination of eddy-current fields using shielded gradients is limited by the manufacturing accuracy, rather than the design accuracy. Also, shielded gradients do not reduce eddy-current fields induced in lossy structures inside the gradient bore. This is possibly the reason for the problems concerning residual eddy-current fields which still occur when a shielded gradient coil is employed (*36, 37*). Additional efforts are essential in shielded gradient systems to compensate for the effects of remaining eddy-current fields originating from imperfect nulling of the pulsed field outside the gradient bore and from inevitable eddy-current fields induced in the interior of the gradient bore. These problems can be handled by additional adjustment of the rephasing gradient waveforms for each experiment (*37*), or by data processing (*36*) using an experiment-specific phase function, similar to the correction of z_0 eddy-current fields (*17*). In some systems shielded gradients are inserted

with a diameter much smaller than that of the magnet bore. This is a rather unsatisfactory use of expensive wide-bore magnets, imposed by the necessity of eliminating the eddy-current fields.

The preemphasis method, on the other hand, has the disadvantage of causing an increased boil-off of cryogens due to the joule heating induced by the eddy currents in the Dewar. This effect will be small (depending on the construction of the superconducting magnet and on the measurement techniques used) and of no great importance when a cryocooler is installed. The stability of the preemphasis method depends on the electronic components used in the compensation circuit, and on the temperature changes of, e.g., cryostat shields. Therefore, care must be taken with the choice of the hardware components, which must be stable over time and with respect to the environment temperature, and with the design of the magnet in order to minimize the temperature changes of the cryostat shields in which eddy currents are induced, since this would result in changes in the resistivity and therefore in the time constants of the induced eddy-current fields (*7*).

It is not possible to compensate cross terms in systems without higher-order or z_0 shims, or with shim coils and amplifiers which cannot be operated dynamically. In that case the best result is obtained by optimizing the compensation separately for several smaller volumes, instead of one large volume covering the complete region of interest, and assembling correction filters for each small volume. Then, for NMR spectroscopy or imaging which is located dominantly over such a smaller volume, the corresponding compensation circuit must be used. Alternatively, when a computer-controlled compensation circuit is implemented, look-up tables with the compensation constants for each small volume can be employed.

Both shielded gradients and preemphasis methods require about the same gradient amplifier power for gradient sets which are optimally designed, are equally strong, have a similar linearity over the same region of interest, and have the same diameter for the free bore. The additional power over a situation without any shielding or compensation of eddy-current fields is, in the case of preemphasis, used for the decaying overshoot, and in the case of shielding, continuously used to compensate for the opposing field generated by the screening gradient (employed to null the gradient field outside the gradient tube) over the region of interest.

CONCLUSION

We have demonstrated a method for complete quantitative characterization and exact temporal and spatial compensation of eddy-current fields, including eddy-current fields with z_0 or any other spatial symmetry q different from that of the pulsed gradient p. The required correction can be calculated exactly from the multiexponentially decaying step response measured without compensation using a large phantom. For diagonal terms ($q = p$) the correction is given by the inverse of the diagonal transfer function of the system. The compensation is described by the same number of exponentials as the diagonal step response of the system, but with different amplitudes and time constants. For cross terms ($q \neq p$) the correction is given by the negative of the nondiagonal transfer function of the system, when implemented according to scheme (a) in Fig. 4. The compensation is described by the same number of expo-

nentials as the cross-term step response of the system, with the same (but negative) amplitudes and the same time constants.

It is evident that when the presented compensation algorithm is combined with self-shielded gradients, the final suppression of eddy-current effects will be improved optimally. As an upgrade of available unshielded gradient coils, the proposed compensation method is a minor technical modification yielding a major improvement in the performance of the system. It is comprehensive, straightforward, and easy and inexpensive to implement and gives a superior suppression of the eddy-current effects during and following gradient pulses.

ACKNOWLEDGMENTS

The help of Drs. R. P. van Stapele and Dr. Q. H. F. Vrehen with the theoretical calculations is gratefully acknowledged. The authors express their gratitude to Mr. J. H. den Boef, Ing. H. J. van den Boogert, Dr. J. Konijn, and Ing. K. Oostveen for stimulating discussions and to Dr. H. Bomsdorf and Dr. W. M. M. J. Bovée for communicating their preliminary results with our algorithm on the compensation of eddy currents in a 4 T human whole-body system and a 7 T vertical-bore animal system, respectively.

REFERENCES

1. R. M. HENKELMAN AND M. J. BRONSKILL, *Rev. Magn. Reson. Med.* **2,** 1 (1987).
2. W. P. AUE, *Rev. Magn. Reson. Med.* **1,** 21 (1986).
3. W. R. SMYTHE, "Static and Dynamic Electricity," 3rd ed., Chap. X, pp. 368–414, McGraw-Hill, New York, 1968.
4. R. L. STOLL, "The Analysis of Eddy Currents," Clarendon Press, Oxford, England, 1974.
5. C. P. BEAN, R. W. DEBLOIS, AND L. B. NESBITT, *J. Appl. Phys.* **30,** 1976 (1959).
6. J. LAPAGE, A. BERNALITE, AND D. A. LINDHOLM, *Rev. Sci. Instrum.* **39,** 1019 (1968).
7. G. R. MORROW AND C. H. ROSNER, *IEEE Trans. Magn.* **MAG-23,** 1294 (1987).
8. A. G. COLLINS, D. RODGER, J. F. EASTHAM, P. J. LEONARD, D. J. BRYANT, AND I. R. YOUNG, "Society of Magnetic Resonance in Medicine; Eighth Annual Meeting and Exhibition, Amsterdam, The Netherlands, August 12–18, 1989, Book of Abstracts," Vol. 2, p. 967.
9. R. D. PILLSBURY AND W. F. PUNCHARD, *IEEE Trans. Magn.* **MAG-21,** 2273 (1985).
10. R. TURNER AND R. M. BOWLEY, *J. Phys. E* **19,** 876 (1986).
11. P. MANSFIELD AND B. CHAPMAN, *J. Phys. E* **19,** 540 (1986).
12. P. B. ROEMER, W. A. EDELSTEIN, AND J. S. HICKEY, "Society of Magnetic Resonance in Medicine, Fifth Annual Meeting, Montreal, Quebec, Canada, August 19–22, 1986, Book of Abstracts," Vol. 3, p. 1067.
13. B. CHAPMAN AND P. MANSFIELD, *J. Phys. D* **19,** L129 (1986).
14. M. A. MORICH, D. A. LAMPMAN, W. R. DANNELS, AND F. T. D. GOLDIE, *IEEE Trans. Med. Imaging* **7,** 247 (1988).
15. P. JEHENSON, M. WESTPHAL, AND N. SCHUFF, "Society of Magnetic Resonance in Medicine, Eighth Annual Meeting and Exhibition, Amsterdam, The Netherlands, August 12–18, 1989, Book of Abstracts," Vol. 2, p. 966.
16. D. J. JENSEN, W. W. BREY, J. L. DELAYRE, AND P. A. NARAYANA, *Med Phys.* **14,** 859 (1987).
17. R. J. ORDIDGE AND I. D. CRESSHULL, *J. Magn. Reson.* **69,** 151 (1986).
18. P. JEHENSON AND A. SYROTA, *Magn. Reson. Med.* **12,** 253 (1989).
19. G. H. GLOVER, "28th Experimental NMR Conference, Asilomar, California, April 5–9, 1987, Book of Abstracts."
20. I. M. BRERETON, J. FIELD, L. N. MOXON, M. G. IRVING, AND D. M. DODDRELL, *Magn. Reson. Med.* **9,** 118 (1989).
21. A. V. OPPENHEIM AND A. S. WILLSKY, with I. T. YOUNG, "Signals and Systems," Prentice-Hall, Englewood Cliffs, New Jersey, 1983.
22. R. N. BRACEWELL, "The Fourier Transform and Its Applications," Chap. 11, McGraw-Hill, Kogakusha, Japan, 1983.

23. F. ROMÉO AND D. I. HOULT, *Magn. Reson. Med.* **1,** 44 (1984).
24. L. BRATEMAN, T. T. BOWMAN, S. DØNSTRUP, AND K. N. SCOTT, *Magn. Reson. Med.* **6,** 459 (1988).
25. T. DUCZMAL, J. KUBIAK, H. A. BUCKMASTER, AND P. MILLIGAN, *J. Magn. Reson.* **77,** 471 (1988).
26. J. J. VAN VAALS, J. H. DEN BOEF, A. H. BERGMAN, AND A. HEERSCHAP, *in* "Proceedings, Second European Congress of NMR in Medicine and Biology, Berlin, FRG, June 23–26, 1988," p. P155.
27. J. J. VAN VAALS, J. H. DEN BOEF, AND A. H. BERGMAN, "Society of Magnetic Resonance in Medicine, Seventh Annual Meeting and Exhibition, San Francisco, California, August 20–26, 1988, Book of Abstracts," Vol. 2, p. 950.
28. J. J. VAN VAALS, A. H. BERGMAN, H. J. VAN DEN BOOGERT, AND A. HEERSCHAP, "NMR Spectroscopy in Vivo—ICR 89 Satellite Congress, Lyon, France, July 10–12, 1989, Book of Abstracts," p. 66.
29. J. J. VAN VAALS, A. H. BERGMAN, H. J. VAN DEN BOOGERT, A. HEERSCHAP, A. J. VAN DER KOGEL, A. C. C. RUIFROK, AND H. J. BERNSEN, "Society of Magnetic Resonance in Medicine, Eighth Annual Meeting and Exhibition, Amsterdam, The Netherlands, August 12–18, 1989, Book of Abstracts," Vol. 1, p. 144.
30. J. J. VAN VAALS, A. H. BERGMAN, H. J. VAN DEN BOOGERT, P. H. J. VAN GERWEN, AND A. HEERSCHAP, "Society of Magnetic Resonance in Medicine, Eighth Annual Meeting and Exhibition, Amsterdam, The Netherlands, August 12–18, 1989, Book of Abstracts," Vol. 1, p. 244.
31. J. J. VAN VAALS, Dutch Patent Application NL 8802212 (1988).
32. Y. S. KIM, D. H. KANG, J. H. KIM, Z. H. CHO, AND J. B. RA, "Society of Magnetic Resonance in Medicine, Seventh Annual Meeting and Exhibition, San Francisco, California, August 20–26, 1988, Book of Abstracts," Vol. 1, p. 29.
33. B. CHAPMAN, R. TURNER, R. J. ORDIDGE, M. DOYLE, M. CAWLEY, R. COXON, P. GLOVER, AND P. MANSFIELD, *Magn. Reson. Med.* **5,** 246 (1987).
34. P. A. BOTTOMLEY, H. C. CHARLES, P. B. ROEMER, D. FLAMIG, H. ENGESETH, W. A. EDELSTEIN, AND O. M. MUELLER, *Magn. Reson. Med.* **7,** 319 (1988).
35. R. TURNER, B. CHAPMAN, A. M. HOWSEMAN, R. J. ORDIDGE, R. COXON, P. GLOVER, AND P. MANSFIELD, *J. Magn. Reson.* **80,** 248 (1988).
36. R. J. ORDIDGE, A. HOWSEMAN, R. COXON, R. TURNER, B. CHAPMAN, P. GLOVER, M. STEHLING, AND P. MANSFIELD, *Magn. Reson. Med.* **10,** 227 (1989).
37. P. C. M. VAN ZIJL, C. T. W. MOONEN, J. R. ALGER, J. S. COHEN, AND S. A. CHESNICK, *Magn. Reson. Med.* **10,** 256 (1989).